Research on Multi-Scenario Planting Optimization Based on WSN Technology and Improved Genetic Algorithm

Qi Liu*

School of Electronic and Information Engineering, Beijing Jiaotong University, Beijing, China, 100091

*Corresponding author: 22723011@bjtu.edu.cn

Abstract. This research focuses on the optimization of agricultural planting, aiming to enhance agricultural production efficiency and maximize planting profits. The research adopts a method of deep integration of 5G, Wireless Sensor Network (WSN), and an improved genetic algorithm. By using 5G and WSN communication technologies, environmental data of various plots, including greenhouses, arid lands, and terraced fields, are collected in real time and stably transmitted to the data processing terminal, providing comprehensive and accurate information support for planting decisions. Meanwhile, the elite retention strategy and immigration strategy are introduced to improve the traditional genetic algorithm, and the improved genetic algorithm is used to solve the optimization problem of planting strategies under multiple constraints. The results show that this method significantly increases planting profits. Under different market scenarios, the annual profit has a remarkable growth, and the centralized management profit increases the total profit by approximately 5 - 6%. The research proves that this model provides scientific and efficient decision - making support for multi - scenario planting management and effectively promotes the intelligent development of agricultural production.

Keywords: WSN, Crop Planting Optimization, Improved Genetic Algorithm, 5G Communication Technology, Multi-constraint Model.

1. Introduction

With the advancement of the global digital wave, communication technologies are integrating into various industries at an unprecedented pace, and the agricultural sector is no exception. Advanced communication technologies such as Wireless Sensor Networks (WSNs) and 5G have brought revolutionary changes to agricultural production [1].

In recent years, scholars have conducted diverse research on agricultural planting. Xiao Pengfei and Peng Sen proposed applying 5G communication technology to agricultural planting to provide precise guidance for crop planting and growth [2]. Zhu Yali proposed a smart agricultural planting system based on the integration of NFC and the Internet of Things to achieve intelligent crop planting and sales [3].

However, existing research still has many limitations. In the research on the application of communication technologies in smart agriculture, there is relatively little research on the collaborative work of multiple communication technologies, and the measures to ensure communication security and stability are not comprehensive enough. In addition, the research on the application of 5G in agricultural planting needs to be further explored in terms of long - term cost - benefit analysis and network coverage stability.

To address the above - mentioned issues, this research proposes a multi - scenario planting optimization scheme that integrates communication technologies and an improved genetic algorithm. Through a more comprehensive sensor layout and advanced communication technologies, the environmental data of multiple planting scenarios are collected and transmitted in real - time and accurately to ensure the integrity and timeliness of information. The improved genetic algorithm is used to incorporate multiple practical constraints into the model, such as environmental differences among different plots, time - series requirements for crop growth, and dynamic changes in market supply and demand, effectively solving the optimization problem of planting strategies under multiple constraints and dynamic changes.

2. Data Collection and Transmission Based on WSN

In various agricultural plots such as smart greenhouses, arid lands, terraced fields, sloping fields, and irrigated fields, the wireless sensor network is responsible for collecting environmental data that is crucial to crop growth. Due to the unique geographical conditions and planting characteristics of different types of plots, there are specific focuses in the selection and layout of sensors.

2.1. Sensor Selection and Layout

(1) Smart Greenhouses

To achieve precise monitoring of the environment inside the smart greenhouse, high - precision and high - stability temperature and humidity sensors are adopted. The temperature measurement range of these sensors is from - 20°C to 85°C, with a measurement accuracy of up to ±0.5°C and a resolution of 0.01°C. The relative humidity measurement range is from 0 to 100% rh, with an accuracy of ±4.5% rh and a resolution of 0.1% rh. In terms of layout, a sensor is arranged every 10 meters to ensure that subtle changes in temperature and humidity within the greenhouse can be accurately captured. In addition, light sensors are deployed in areas where the light intensity changes significantly and above the crop canopy. Their measurement range is from 1 lux to 65535 lux, with a measurement accuracy of ±0.5% and a resolution of 0.1 lux. One sensor is set every 20 square meters to accurately measure the light intensity. Carbon dioxide sensors with a measurement range of 1 ppm to 20 kppm, a measurement accuracy of ±30 ppm, and a resolution of 1.00 ppm are selected. These sensors are evenly distributed in the greenhouse, with one installed every 50 square meters. Based on the principle of infrared double - beam, these sensors are encapsulated in a louver - box - shaped housing, which has good air permeability and waterproof properties, ensuring the stability of the measured data.

(2) Arid Farmlands

The monitoring of arid farmlands focuses on soil moisture content and meteorological condition parameters. Therefore, professional soil moisture monitoring equipment is used, which can accurately measure the soil water content at different depths. The measurement range is from 0 to 100% rh, with an accuracy of up to ±5% rh, providing crucial data support for precise irrigation in arid farmlands.

(3) Terraced and Sloping Farmlands

Due to the complex terrain of terraced and sloping farmlands, there is a high risk of soil erosion. Therefore, professional soil erosion monitors are arranged on the ridges of terraced fields and the slopes of sloping farmlands to monitor the soil erosion situation in real - time, so that corresponding soil and water conservation measures can be taken in a timely manner.

2.2. Signal Processing

The analog signals collected by sensors are usually weak and may be mixed with noise. Therefore, moving average filtering is used for noise reduction, that is, the arithmetic mean of N continuously collected temperature data is calculated to obtain the filtered temperature value.

$$\mathrm{y}_n = \frac{1}{N}\sum_{i=n-N+1}^{n} x_i \tag{1}$$

where y_n is the output value after the n -th filtering, x_i is the temperature data collected at the i -th time, and N is the number of data points involved in the averaging.

The temperature analog signal $V_{in}(t)$ after the previous noise - reduction processing enters the analog - to - digital conversion (ADC) stage. In this stage, oversampling technology is adopted for further noise reduction. Let the original Nyquist sampling rate be f_N . After K -fold oversampling, the sampling rate becomes $f_{os} = Kf_N$. In terms of noise power, the noise power before oversampling is P_n , and the noise power $P_{n,os}$ after oversampling satisfies the formula

$$P_{n,os} = \frac{P_n}{K} \tag{2}$$

Thus achieving further noise reduction of the temperature signal, improving the signal quality, and providing a more reliable analog - signal input for the subsequent conversion into a digital signal.

2.3. Data Transmission and Processing Algorithms

The analog signals collected by sensors are converted and then transmitted to the aggregation nodes via low - power wireless communication protocols such as ZigBee and LoRa [4]. In the smart greenhouse, sensors and aggregation nodes are reasonably arranged according to the greenhouse structure to effectively avoid obstacles and ensure the smoothness of the communication link. In the outdoor environment, due to the long distance and the easy attenuation of signals, relay nodes are added to enhance the signal strength and ensure the stability of long - distance transmission.

The aggregation nodes collect data from various sensors and perform preliminary processing. Among them, the Kalman filter algorithm and the wavelet transform algorithm play important roles in data processing.

2.3.1 Kalman Filter Algorithm

The Kalman filter is based on the state equation of a linear system. Through prediction and update steps, it fuses the system's input and output observation data to optimally estimate the system state. In the smart farmland, environmental data are interfered by various factors. This algorithm can handle uncertainties and fuse multi - source sensor data, such as integrating the relationships among variables like temperature, humidity, light, and carbon dioxide concentration, accurately estimate the environmental state, and assist in planting decision - making.

2.3.2 Wavelet Transform Algorithm

The wavelet transform uses a set of wavelet functions to translate and scale signals and analyze signals at different scales, with good time - frequency localization characteristics. Compared with the traditional Fourier transform, it can locate the time position of frequency components. In the farmland, light data are often noisy due to weather and other factors. This algorithm can separate noise from real signals, retain light change information, and contribute to the study of the relationship between crop photosynthesis and light conditions.

Through communication technologies, a wealth of environmental data is obtained in this study. Based on these environmental data, the DSSAT model is used to predict the yield per mu [5][6], the linear regression model is used to evaluate the planting cost [7], and a combined model of time - series analysis and neural networks is used to predict the unit sales price and other key parameters required for optimizing the planting strategy are simulated and generated [8].

3. Research on the Construction of Crop Planting Optimization Model and Scenario Strategies Based on Communication Technology

This study solves the problem under two scenarios, and the core difference lies in the handling of the part where the yield exceeds expectations in the objective function.

In the unsalable scenario, the actual sales volume is calculated as the minimum value between the expected sales volume and the planted yield to calculate the sales revenue. In the price-reduction selling scenario, when the planted yield is less than the expected sales volume, all products are sold at the normal price, and for the part that exceeds the expected sales volume, they are sold at half price to calculate the revenue.

To maximize the planting revenue and take into account the convenience of management, a planning model is constructed. Taking the planting area of crops in each plot as the decision-making variable, the objective function comprehensively considers the potential revenue, decentralized management costs, and centralized management revenue to maximize the total revenue. The constraint conditions cover plot area, crop type, and planting time limitations.

3.1. Data Pre-processing

There are 6 types of plots, namely arid land, terraced fields, hillside land, irrigated land, ordinary greenhouses, and smart greenhouses. Considering that irrigated land and greenhouses can be used to plant two seasons of crops, for the convenience of calculation, the number of these plots is respectively doubled. Therefore, there are a total of 82 plots, and the plots are represented by the letter i, that is, $i = 1, 2, ..., 82$. There are three major categories of crops, namely grains, vegetables, and edible fungi. Grains and vegetables include several types of legumes, with a total of 41 varieties, and the crops are represented by the letter j, that is, $j = 1, 2, ..., 41$. Taking 2023 as the base year, the crop-planting strategies from 2024 to 2030 are optimized, and the years are represented by the letter k, that is, $k = 1, 2, ..., 7$. Figure 1 below gives a detailed description of the definition of plot numbers in this paper.

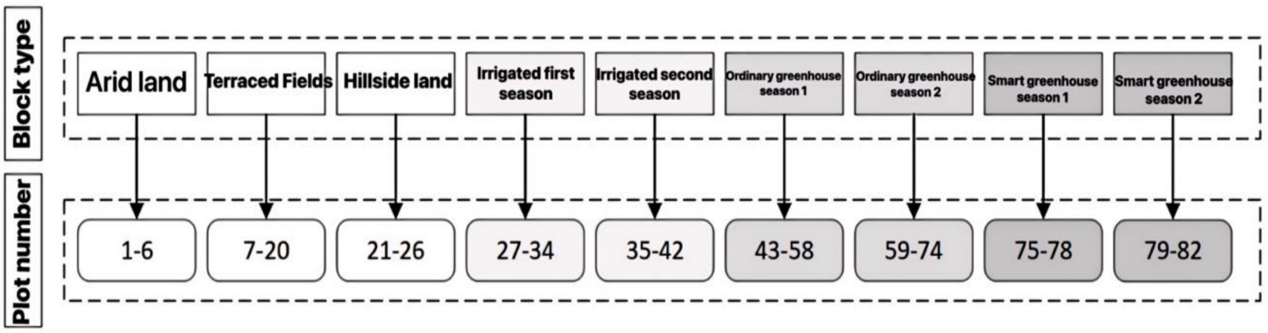

Figure 1. Plot number description

First, parameters such as per-mu yields, planting costs, and sales unit prices are converted into matrix data of 82×41. Then, descriptive statistical analysis is carried out on some of the parameters. Figure 2 shows the yield situation of 41 types of crops in 2023.

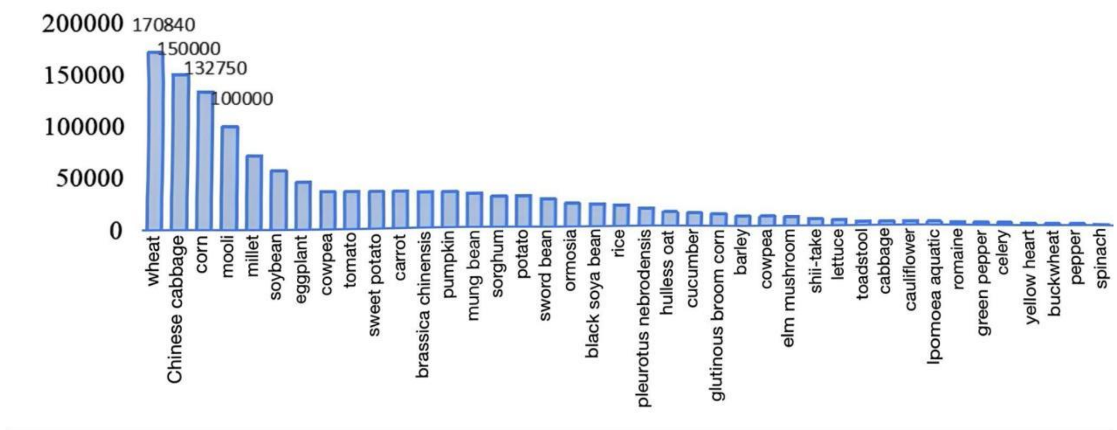

Figure 2. Crop yield in 2023

The crop yield data in 2023 shows that wheat ranks first with a yield of 170,800 jin. The yields of Chinese cabbage, corn, and white radish all exceed 100,000 jin. In contrast, the yields of crops such as spinach, chili peppers, buckwheat, celery, and yellow-heart cabbage are relatively low, less than 2,000 jin. In the future, under the baseline scenario, the market will continue this trend. Based on the above-mentioned situation, this study makes the following assumption: During the period from 2024 to 2030, the expected sales volume of each type of crop is equal to the yield of each type of crop in 2023.

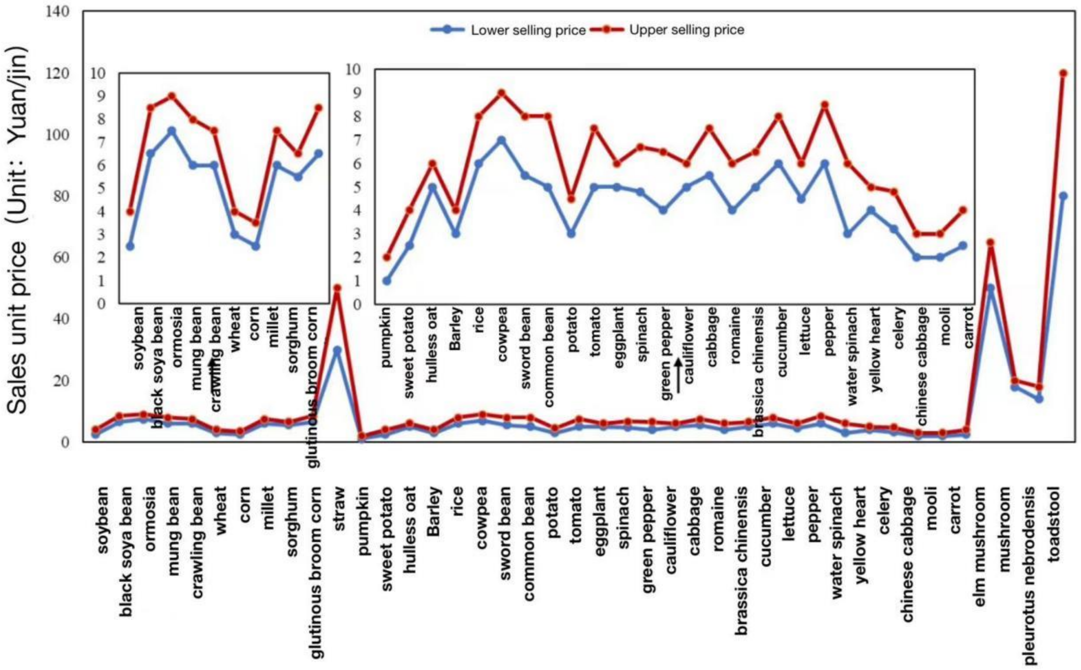

Figure 3. The unit sales prices of crops in 2023

Subsequently, this study conducts a statistical analysis of the unit sales prices of 41 crops in 2023. Figure 3 shows the unit sales prices of these crops in 2023. The blue line represents the lower limit of the unit price, and the red line represents the upper limit of the selling price. Among them, mushroom-type crops such as Morchella have high unit prices, while grain-type crops such as wheat and pumpkin have low unit prices. Moreover, the price-floating ranges of various crops vary significantly. In view of this, in-depth research on how to optimize crop-planting strategies is warranted.

3.2. Optimization Model of Crop Planting Strategies under the Scenario of Unsold Excess Yield

3.2.1 Construction of the Objective Function

The objective function is to maximize the cumulative planting revenue from 2023 to 2030. The total revenue consists of three parts: sales revenue, planting cost, and centralized management revenue. Among them, the centralized management revenue is determined by the planting concentration. In this paper, the planting concentration is defined as follows:

$$The\_planting\_concentretion = \frac{\sum_i x_{i,j}^k}{\sum_i q_{i,j}^k} \tag{3}$$

$$x_{i,j}^k, i = 1, 2, ..., 82; \ j = 1, 2, ..., 41; k = 1, 2, ..., 7 \tag{4}$$

Among them, $x_{i,j}^k$ represents the area of the j-th crop planted on the i-th plot in the k-th year.

In the above formula, the planting concentration is obtained by dividing the planting area of a certain crop by the number of plots on which it is planted. The calculation formulas for other parts are as follows:

$$R' = \sum_{i,j,k} [S_j (\sum_i P_{i,j}^k x_{i,j}^k w - \sum_i P_{i,j}^k y_{i,j}^k (1-w))] \tag{5}$$

$$C_1 = C_{i,j}^k x_{i,j}^k \tag{6}$$

$$V=\sum_{j,k}\frac{\sum_{i}x_{i,j}^{k}}{\sum_{i}q_{i,j}^{k}}\lambda_{c} \tag{7}$$

Among them, R' represents the sales revenue, which is obtained by multiplying the per-mu yield, unit price, and planting area. Here, it is considered that the part of the yield exceeding the expected sales volume will cause unsalable products, that is, the sales volume is taken as the minimum of the two, and this relationship is depicted by introducing a 0-1 variable w. C_1 represents the inherent planting cost, which is obtained by multiplying the unit planting cost and the planting area, depicting the fixed cost of planting. V represents the centralized management revenue, depicting the practical problem that a high degree of planting concentration is convenient for operations and field management. In the formula, $S_{i,j}^{k}$ represents the sales price of the crop, $P_{i,j}^{k}$ represents the per-mu yield of the crop, $y_{i,j}^{k}$ represents the expected sales volume of a certain crop, $C_{i,j}^{k}$ represents the planting cost of a certain crop on a certain plot, and λ_c represents the unit centralized management revenue. In summary, the objective function of this optimization model is as follows:

$$\max R_{1}=\sum_{i,j,k}[S_{j}(\sum_{i}P_{i,j}^{k}x_{i,j}^{k}w-\sum_{i}P_{i,j}^{k}y_{i,j}^{k}(1-w))]-C_{i,j}^{k}x_{i,j}^{k}-\sum_{j,k}\frac{\sum_{i}x_{i,j}^{k}}{\sum_{i}q_{i,j}^{k}}\lambda_{c} \tag{8}$$

3.2.2 Setting of Constraint Conditions

(1) Constraints on the Planting Area of Plots

Each plot has a maximum available area, which is the upper-limit of the crop-planting area.

$$\sum_{j}x_{i,j}^{k}\leq land_{i}^{k},i=1,2,...,82;k=1,2,...7 \tag{9}$$

The above formula indicates that in a certain year, the total planting area of all crops on a certain plot does not exceed the available area of that plot. $land_i^k$ represents the available area of the i-th plot in the k-th year.

(2) Constraints on the Crop Types Planted in Each Plot

Four types of plots are considered in the model. Different crops have different requirements for land types, and the detailed constraints are as follows.

a. Planting restrictions for arid land, terraced fields, and hillside-type plots

$$\sum_{i=1}^{26}\sum_{j=16}^{41}x_{i,j}^{k}=0,k=1,2,...7 \tag{10}$$

The above formula indicates that crops numbered 16-41 cannot be planted in these three types of plots, namely arid land, terraced fields, and hillside land.

b. Planting restrictions for irrigated land plots

$$\sum_{i=27}^{42}\sum_{j=1}^{15}\sum_{j=38}^{41}x_{i,j}^{k}=0,k=1,2,...,7 \tag{11}$$

The above formula indicates the crops that cannot be planted in irrigated land. Whether in the first or second season, crops numbered 1-15 and 38-41 cannot be planted in irrigated land.

$$\begin{cases} \sum_{i=35}^{42} x_{i,j}^k = 0, if \sum_{i=27}^{34} x_{i,16}^k > 0, \forall j, k \\ \sum_{i=27}^{34} \sum_{j=1}^{16} \sum_{j=35}^{41} x_{i,j}^k + \sum_{i=35}^{42} \sum_{j=1}^{34} \sum_{j=38}^{41} x_{i,j}^k = 0, if \sum_{i=27}^{34} x_{i,16}^k = 0, \forall k \end{cases} \tag{12}$$

The above formula indicates that if rice is planted in the first season in irrigated land, it cannot be planted again in the second season; if vegetables are planted instead of rice in the first season, then two-season planting is possible. Also, crops numbered 1-16 and 35-41 cannot be planted in the first season, and crops numbered 1-34 and 38-41 cannot be planted in the second season.

c. Planting restrictions for ordinary greenhouses

$$\sum_{i=43}^{58} \sum_{j=1}^{16} \sum_{j=35}^{41} x_{i,j}^k = 0, k = 1, 2, \ldots 7 \tag{13}$$

The above formula indicates that crops numbered 1-16 and 35-41 cannot be planted in the first season in ordinary greenhouses.

$$\sum_{i=59}^{74} \sum_{j=1}^{37} x_{i,j}^k = 0, k = 1, 2, \ldots 7 \tag{14}$$

The above formula indicates that crops numbered 1-37 cannot be planted in the second season in ordinary greenhouses, and only crops numbered 38-41 can be planted.

d. Planting restrictions for smart greenhouses

$$\sum_{i=75}^{82} \sum_{j=1}^{16} \sum_{j=35}^{41} x_{i,j}^k = 0, k = 1, 2, \ldots 7 \tag{15}$$

The above formula indicates that crops numbered 1-16 and 35-41 cannot be planted in either the first or second season in smart greenhouses, and only crops numbered 38-41 can be planted.

(3) Constraints on crop-planting time

The model takes 2023 as the base year for the optimization model and makes plans for 2024-2030. The constraints set for the time requirements of crop planting are as follows.

a. Restrictions on crop-growth rules

$$x_{i,j}^k x_{i,j}^{k+1} = 0, k = 0, 1, \ldots 6, \forall i, j \tag{16}$$

The above formula indicates that the same type of crop cannot be continuously planted in the same plot for two consecutive years to avoid yield reduction. In the above formula, $x_{i,j}^0$ represents the crop-planting situation in 2023. Since this constraint is a non-linear constraint, it is transformed into a linear constraint by introducing 0-1 variables, and the formula is as follows:

$$\begin{cases} x_{i,j}^k \le land_{i,j}^k m_{i,j}^k \\ x_{i,j}^{k+1} \le land_{i,j}^{k+1} n_{i,j}^k \\ m_{i,j}^k + n_{i,j}^k \le 1 \\ k = 0, 1, \ldots, 6 \end{cases} \tag{17}$$

In the above formula, $m_{i,j}^k$ and $n_{i,j}^k$ are 0-1 variables, and $land_{i,j}^k$ represents the maximum available area of the plot.

b. Constraints on legume-crop planting

Since the soil containing legume-crop roots is beneficial to the growth of other crops, it is required that each plot should plant legume crops at least once within three years starting from 2023. Therefore, the model sets the following constraints:

$$\sum_{j=1}^{5}\sum_{j=17}^{19}(x_{i,j}^{k-1}+x_{i,j}^{k}+x_{i,j}^{k+1})>0,\forall i,k=1,2,...,6 \tag{18}$$

In the above formula, numbers 1-5 and 17-19 represent legume crops, indicating that starting from 2023, each plot should plant legume crops at least once within three years.

(4) Linear-transformation constraints for production-sales comparison

Since the objective function needs to compare the yields and sales volumes of crops, this paper introduces a 0-1 variable w to depict the relationship between the two (taking the smaller value of the two as the sold quantity). The formulas are as follows:

$$x_{i,j}^{k}P_{i.j}^{k}-y_{i,j}^{k}>(w-1)M \tag{19}$$

$$x_{i,j}^{k}P_{i.j}^{k}-y_{i,j}^{k}\le wM \tag{20}$$

In the above formulas, M represents an infinitely large value, and 1020 is used to replace it in the code.

(5) Linear-transformation constraints for the index of decentralized management costs

The index of planting concentration is required in the decentralized management costs, which is achieved through the following constraints:

$$x_{i,j}^{k}>(q_{i,j}^{k}-1)M \tag{21}$$

$$x_{i,j}^{k}\le q_{i,j}^{k}M \tag{22}$$

In the above formulas, M represents an infinitely large value, and 1020 is used to replace it in the code.

(6) Other constraints

The planting area of crops is non-negative, and the constraints on 0-1 variables are as follows.

$$x_{i,j}^{k}\ge 0 \tag{23}$$

$$w_{i,j}^{k},q_{i,j}^{k},m_{i,j}^{k},n_{i,j}^{k}\in\{0,1\} \tag{24}$$

3.2.3 Model Summary

In summary, the optimized crop-planting strategy model constructed in this paper is as follows (for the scenario of unsold excess yield):

$$\max R_1=\sum_{i,j,k}[S_j(\sum_{i}P_{i,j}^{k}x_{i,j}^{k}w-\sum_{i}P_{i,j}^{k}y_{i,j}^{k}(1-w))]-C_{i,j}^{k}x_{i,j}^{k}-\sum_{j,k}\frac{\sum_{i}x_{i,j}^{k}}{\sum_{i}q_{i,j}^{k}}\lambda_c \tag{25}$$

$$
s.t.\begin{cases}
\sum_{j} x_{i,j}^{k} \le land_{i}^{k}, i=1,2,...,82; k=1,2,...7 \\
\sum_{i=1}^{26}\sum_{j=16}^{41} x_{i,j}^{k} = 0, k=1,2,...7 \\
\sum_{i=27}^{42}\sum_{j=1}^{15}\sum_{j=38}^{41} x_{i,j}^{k} = 0, k=1,2,...,7 \\
\sum_{i=35}^{42} x_{i,j}^{k} = 0, if \sum_{i=27}^{34} x_{i,16}^{k} > 0, \forall j,k \\
\sum_{i=27}^{34}\sum_{j=1}^{16}\sum_{j=35}^{41} x_{i,j}^{k} + \sum_{i=35}^{42}\sum_{j=1}^{34}\sum_{j=38}^{41} x_{i,j}^{k} = 0, if \sum_{i=27}^{34} x_{i,16}^{k} = 0, \forall k \\
\sum_{i=43}^{58}\sum_{j=1}^{16}\sum_{j=35}^{41} x_{i,j}^{k} = 0, k=1,2,...7 \\
\sum_{i=59}^{74}\sum_{j=1}^{37} x_{i,j}^{k} = 0, k=1,2,...7 \\
\sum_{i=75}^{82}\sum_{j=1}^{16}\sum_{j=35}^{41} x_{i,j}^{k} = 0, k=1,2,...7 \\
x_{i,j}^{k} \le land_{i}^{k} m, k=0,1,...,6 \\
x_{i,j}^{k+1} \le land_{i}^{k+1} n, k=0,1,...,6 \\
m+n \le 1 \\
\sum_{j=1}^{5}\sum_{j=17}^{19} (x_{i,j}^{k-1} + x_{i,j}^{k} + x_{i,j}^{k+1}) > 0, \forall i, k=1,2,...,6 \\
x_{i,j}^{k} P_{i.j}^{k} - y_{i,j}^{k} > (w-1)M, \forall i,j,k \\
x_{i,j}^{k} P_{i.j}^{k} - y_{i,j}^{k} \le wM, \forall i,j,k \\
x_{i,j}^{k} > (q-1)M, \forall i,j,k \\
x_{i,j}^{k} \le qM, \forall i,j,k \\
x_{i,j}^{k} \ge 0, \forall i,j,k \\
w_{i,j}^{k}, q_{i,j}^{k}, m_{i,j}^{k}, n_{i,j}^{k} \in \{0,1\}
\end{cases} \tag{26}
$$

3.3. Optimization Model of crop-planting Strategies under the Scenario of Reducing Prices for the Excess Yield

This part of the model takes into account that the part of the yield exceeding the expected sales volume can still be sold at 50% of the market price. Therefore, it has an additional revenue module compared to the basic model. The rest of the settings remain the same, and the objective function is modified as follows:

$$
\max R_2 = \sum_{i,j,k}[S_j(\sum_{i} P_{i,j}^{k} x_{i,j}^{k} w - \sum_{i} P_{i,j}^{k} y_{i,j}^{k}(1-w))] - C_{i,j}^{k} x_{i,j}^{k} - \sum_{j,k}\frac{\sum_{i} x_{i,j}^{k}}{\sum_{i} q_{i,j}^{k}}\lambda_c + \frac{S_{i,j}^{k} P_{i,j}^{k}(x_{i,j}^{k} - y_{i,j}^{k})(1-w)}{2} \tag{27}
$$

3.4. Solving with an Improved Genetic Algorithm Incorporating the Elite-Retention Strategy and the Immigration Strategy

To enhance the global convergence ability of the algorithm, this paper improves the traditional genetic algorithm by introducing the elite-retention strategy and the immigration strategy[9][10]. The elite-retention strategy can preserve the optimal solution in the current generation, and the immigration strategy can effectively prevent the algorithm from falling into local optimal solutions during later-stage operation.

(1) Encoding and Decoding of Feasible Solutions

Encoding is the mapping of feasible solutions to the algorithm's search space, and decoding is the opposite. Appropriate and efficient encoding and decoding affect the quality of model-solving. In view of the characteristics of the model in this study, the research team adopts multi-dimensional array encoding, regarding the decision-variable matrix as a chromosome. Its structure is a three-dimensional matrix, which is consistent with the decision variables. This encoding preserves the structural characteristics of the problem space, but special operators need to be designed to maintain the multi-dimensional structure of the chromosome during crossover and mutation operations.

(2) Generation of the Initial Population

An initial feasible solution is generated as the initial population to reduce the number of unreasonable iterations.

(3) Evaluation of Individual Fitness

The individual fitness is calculated according to the following formula:

$$F(p,m)=\begin{cases} W+\delta_{\min}, if\ \ W+\delta_{\min}>0 \\ 0, \qquad\qquad if\ \ W+\delta_{\min}\le 0 \end{cases} \tag{28}$$

Among them, W is the objective function, and $\delta_{\min}=0.1$.

(4) Selection Operation

This paper adopts a method that combines the proportional-selection operator with the elite-retention strategy for the selection operation. First, the proportional-selection operator is used to screen out some chromosomes for genetic operations to generate offspring. To prevent subsequent genetic operations from destroying the excellent individuals of the parent generation, the elite-retention strategy is used for improvement. The top 10% of the individuals with high fitness in the parent generation are selected to replace the last 10% of the individuals in the offspring generation, ensuring that the excellent individuals are retained during the evolution.

(5) Crossover Operation

The individuals in the population are paired two by two, and for each pair of chromosomes, it is determined whether to perform a crossover operation with a probability of $p_c=0.6$. To ensure that the chromosomes after crossover meet the conditions, the upper-layer chromosomes are crossed with the upper-layer chromosomes, and the lower-layer chromosomes are crossed with the lower-layer chromosomes during the crossover.

(6) Mutation Operation

When performing a mutation operation on the selected individuals with a probability of $p_m=0.01$, mutation points are randomly selected, and the mutation range is restricted by the constraints of the highest replenishment quantity and the highest pricing to reduce the repair of chromosomes after mutation.

(7) Chromosome Repair

Since chromosome repair may be required after crossover and mutation operations to ensure the legality of chromosomes. During the repair, attempts are made to repair the upper-layer and lower-layer chromosomes respectively, but only the chromosomes with high fitness after repair are retained.

(8) Immigration Operation

To prevent the algorithm from falling into a local optimum in the later stage of evolution, this paper introduces the "immigration strategy" for improvement. First, a threshold is set to determine whether the algorithm has premature convergence. If so, excellent external individuals are introduced into the population to ensure population diversity. When the fitness of individuals in the population is similar, the algorithm is prone to premature convergence. Therefore, it can be judged by the variance of individual fitness. The specific formula is as follows:

$$V = \frac{1}{N}\sum_{i=1}^{n}\left|F_i - F_{avg}\right| \tag{29}$$

In the formula, V is the fitness variance of the population; N is the population size; F_i is the fitness of the i-th individual in the population; F_{avg} is the average fitness of the population. When V is less than a certain threshold, the immigration operation is judged to be carried out.

(9) Termination Condition

When the number of iterations of the algorithm reaches the pre-set number of evolution generations, the algorithm terminates.

$$t = T \tag{30}$$

Finally, MATLAB is used for programming and solving.

4. Result Analysis and Discussion

The improved genetic algorithm incorporating the elite-retention strategy and the immigration strategy can be used to obtain the optimal planting strategies under two different objective functions. The following is a visual display and analysis of the optimized results and total revenue.

(1) Comparative Analysis of Revenues under Two Objective Functions

Figure 4 respectively shows the comparison of the annual revenues and the total revenues from 2024 to 2030 of the optimal planting strategies under the two objective functions.

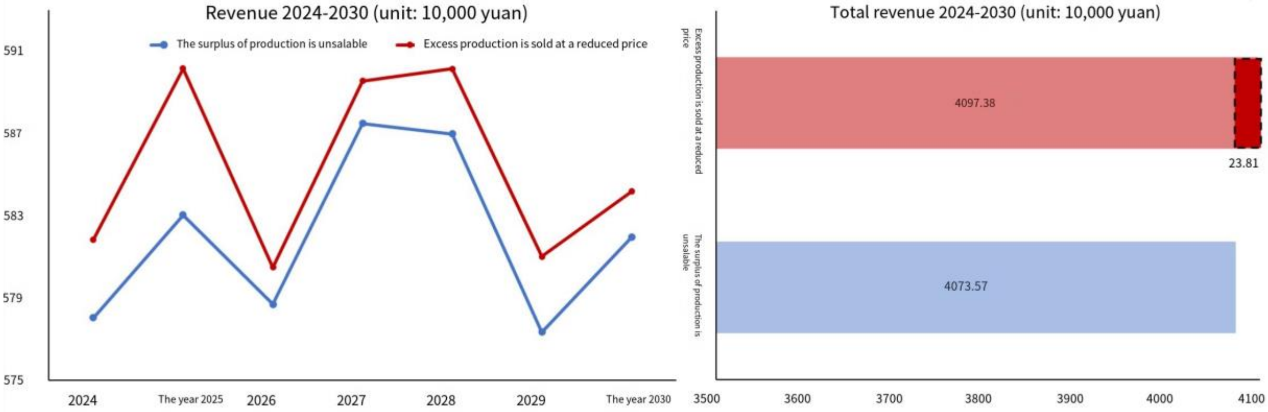

Figure 4. Comparative analysis of the returns under the two objective functions

From the perspective of the annual revenues in Figure 4, the annual revenues under the two objectives fluctuate between 5.75 million and 5.90 million yuan. The annual revenues in the case of price-reduction sales are higher than those in the unsalable scenario every year. From the perspective of the total revenues over seven years, the total revenue in the case of price-reduction sales is 40.9738 million yuan, while that in the unsalable scenario is 40.7357 million yuan, indicating that the price-reduction sales activities will bring an additional revenue of 0.2381 million yuan.

(2) Analysis of Potential Revenues Considering Centralized Management

Figure 5 respectively shows whether the potential centralized management revenues brought about by centralized planting are considered in the objective function under the two sales situations, and compares the planting concentrations of the crops.

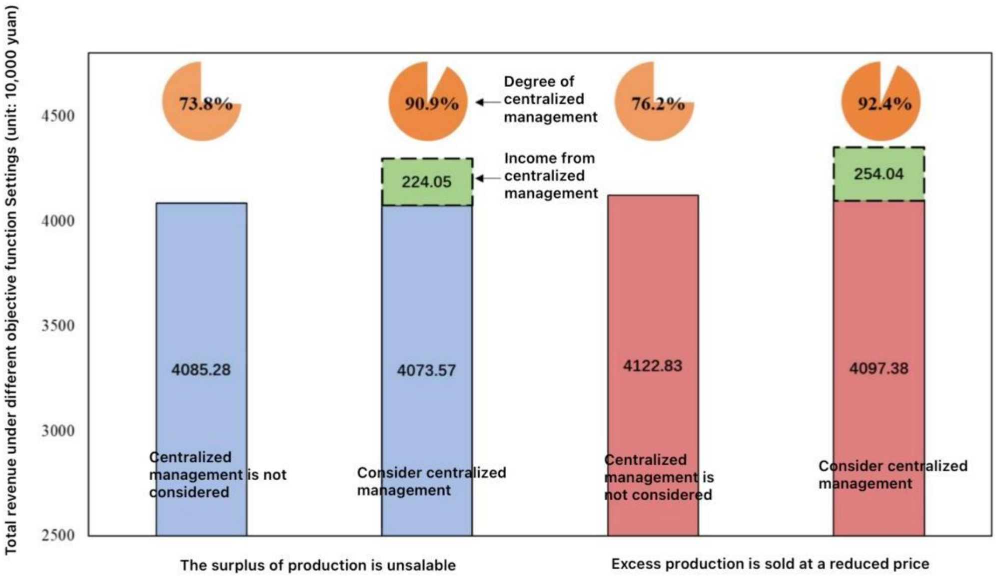

Figure 5. Comparative analysis of centralized management revenue

As can be seen from Figure 5, when centralized management is considered, the crop-planting concentration in the normal-sales scenario increases from 73.8% to 90.9%, generating a centralized management revenue of 2.2405 million yuan, accounting for about 5.5% of the total revenue. In the price-reduction sales scenario, the planting concentration increases from 76.2% to 92.4%, generating a centralized management revenue of 2.5404 million yuan, accounting for about 6.2% of the total revenue. By comparing the two sales scenarios horizontally, whether to consider crop centralized management has a relatively small impact on sales.

In conclusion, adopting a price-reduction sales strategy for the part of the yield exceeding expectations can increase the total revenue, and considering the centralized planting of crops can bring about a centralized-management revenue of about 5-6%. The results of this paper can provide a theoretical reference for future planting and sales strategies.

5. Conclusions

This study has successfully integrated 5G, WSN communication technologies and the improved genetic algorithm in-depth for multi-scenario agricultural planting optimization. The communication technologies enable real time collection and transmission of environmental data from different plots, providing accurate information support for planting decisions. The improved genetic algorithm effectively optimizes planting strategies under multiple constraints, maximizing planting profits. Verified by practical cases, this method has achieved remarkable results in increasing planting profits, optimizing planting strategies, and enhancing centralized management benefits. In the future, with the continuous development of 5G communication technology and the Internet of Things, the method of this study can be further extended to larger - scale agricultural planting scenarios, promoting the development of agricultural production towards intelligence, high - efficiency, and sustainability.

References

[1] Zhu Yali. Research on Smart Agriculture System Based on Internet of Things [J]. Computer Knowledge and Technology, 2020, 16(26): 240 - 241.

[2] Chen Hualin. Exploration of the Application of Telecom Wireless Communication Network in Internet of Things Technology [J]. Electronic Components and Information Technology, 2024, 8(07): 140 - 142.

[3] Xiao Pengfei, Peng Sen. Research on the Application of 5G Communication in Agricultural Planting [J]. Seed Science & Technology, 2019, 37(11): 108 - 109.

[4] Dai Lu, Zhang Min, Xu Long, et al. Design of a Self - powered Sensor System for Smart Agriculture Based on ZigBee Wireless Communication [J]. South China Agricultural Machinery, 2025, 56(01): 49 - 51.

[5] Wu Yuanyuting. Evaluation of the Effects of Nitrogen Application Rate and Film - mulching Cultivation on Wheat Yield in the Loess Plateau Using the DSSAT Model [D]. Northwest A&F University, 2024.

[6] Zhang Puhan. Estimation of Lanzhou Lily Yield Based on the DSSAT Model [D]. Northwest Normal University, 2024.

[7] Suo Panpan. Analysis of the Impact of Temperature on Wheat Yield Based on the Functional Regression Model [D]. Henan University, 2024.

[8] Li Moying. Time - series Analysis Model Based on Multi - source Data [J]. Information Technology, 2025, (01): 112 - 118 + 125.

[9] Gan, G. H., Liu, C. Q., & Yang, D. Research on the optimization of agricultural land structure based on genetic algorithm: A case study of Tongzhou District in Beijing. *Journal of the Graduate School of the Chinese Academy of Sciences*, 2004,21(1), 50 - 55.

[10] Yuan, M., & Liu, Y. L. Land use optimization allocation based on multi-agent genetic algorithm [J]. *Transactions of the Chinese Society of Agricultural Engineering (Transactions of the CSAE)*, 2014,30(1), 191 - 199.